Rapid transport pathways for geothermal fluids in an active Great Basin fault zone

Jerry P. Fairley
Jennifer J. Hinds
Department of Geological Sciences, University of Idaho, Moscow, Idaho 83844-3022, USA

ABSTRACT

We present an analysis of fault hydraulic architecture, based on >700 spatially distributed ground and geothermal spring temperature measurements taken in an active fault zone. Geostatistical simulations were used to extrapolate the measured data over an 800 × 100 m area and develop a high-resolution image of temperatures in the fault. On the basis of the modeled temperatures, a simple analytical model of convective heat transport was used to infer a probability distribution function for hydraulic conductivities in a two-dimensional plane parallel to the land surface, and the partitioning of flow between flow paths of different conductivities was calculated as a fraction of the total flux. The analysis demonstrates the existence of spatially discrete, high-permeability flow paths within the predominantly lower-permeability fault materials. Although the existence of fast-flow paths in faults has been hypothesized for >10 yr, their prevalence and contribution to the total flow of fluid in a fault zone are debated. On the basis of our findings, we conclude that the flux transmitted by an individual fast-flow path is significantly greater than that of an average flow path, but the total flux transported in fast-flow paths is a negligible fraction of the total flux transmitted by the fault.

Keywords: fault hydrology, geothermal, heterogeneity, geostatistics, groundwater.

INTRODUCTION

The way in which faults influence subsurface fluid flow is important in many fields of the earth and planetary sciences, but basic questions regarding the relationships between fluid flow and fault hydraulic architecture remain unanswered. Current conceptual models represent faults as comprising a core of low-permeability gouge, surrounded by a higher-permeability damage zone of fractured rock that grades into undamaged protolith (Caine et al., 1996; Rawling et al., 2001). The properties and extent of the core and damage zones can vary significantly from fault to fault, depending on the host rock, offset, and displacement rate, and in some cases either the core or the damage zone may be absent (Caine et al., 1996; Evans et al., 1997). Although general agreement exists on the outline of this conceptual model, the model does not account for the influence of heterogeneity within the fault, which is thought to be an important control on fluid migration through fault zones (Curewitz and Karson, 1997; Jourde et al., 2002). Field observations suggesting the existence of fast-flow paths that transmit subsurface fluids rapidly over large distances (Fabryka-Martin et al., 1997; Campbell et al., 2003) have demonstrated the need for an improved understanding of the relationship between heterogeneity and subsurface fluid flow; unfortunately, the data necessary to develop such an understanding are difficult to obtain. Fault hydraulic properties are typically extrapolated from point measurements in boreholes (Barton et al., 1995; Kiguchi et al., 2001), from laboratory measurements (Evans et al., 1997; Olsen et al., 1998; Seront et al., 1998), or from observations of surface exposures of inactive faults (Jourde et al., 2002). The data gained from these studies provide important information regarding fault hydraulic properties, but the methods employed are generally not well suited to the acquisition of large data sets from heterogeneous domains.

In order to refine current conceptual models of fault hydraulic architecture and to answer questions regarding the prevalence of fast-flow paths and their role in subsurface fluid transport, a statistically significant number of spatially distributed hydraulic property measurements within a fault zone is required. Here we have used temperature measurements to infer the distribution of fault hydraulic properties in an active normal fault located in the Great Basin subprovince of the western United States. The analysis has yielded the range and spatial distribution of permeability controlling the vertical migration of fluids in the fault, and has allowed the distribution of flux through a horizontal, two-dimensional plane normal to the fault to be quantitatively evaluated.

SITE DESCRIPTION

The extensional terrains of the Great Basin have been the subjects of numerous structural and tectonic investigations. Many of these studies have focused on the interaction between faults and subsurface fluid flow, owing to the high geothermal gradients and active extensional processes that control the location of many geothermal systems within the Great Basin (Coolbaugh et al., 2003). Northwest-southeast–directed bulk regional extension within the Great Basin is manifested along northeast-oriented faults (Blewitt et al., 2003; Pezzopane and Weldon, 1993), and high-temperature geothermal systems in the Great Basin are preferentially associated with these northeast-trending lineaments (Koenig and McNitt, 1983). High-permeability pathways are required to bring geothermal fluids to the land surface at temperatures significantly greater than the surrounding environment (Forster and Smith, 1989; Wisian et al., 1999; Wisian, 2000), and current activity associated with the northeast-trending structures provides higher-permeability conduits for flow in comparison to faults of other orientations.

A number of researchers have examined fluid flow in fault-controlled, geothermal systems; for example, Bruhn et al. (1990, 1994) investigated fracturing and hydrothermal alteration associated with normal faults at Dixie Valley, Nevada, and the Wasatch fault zone in

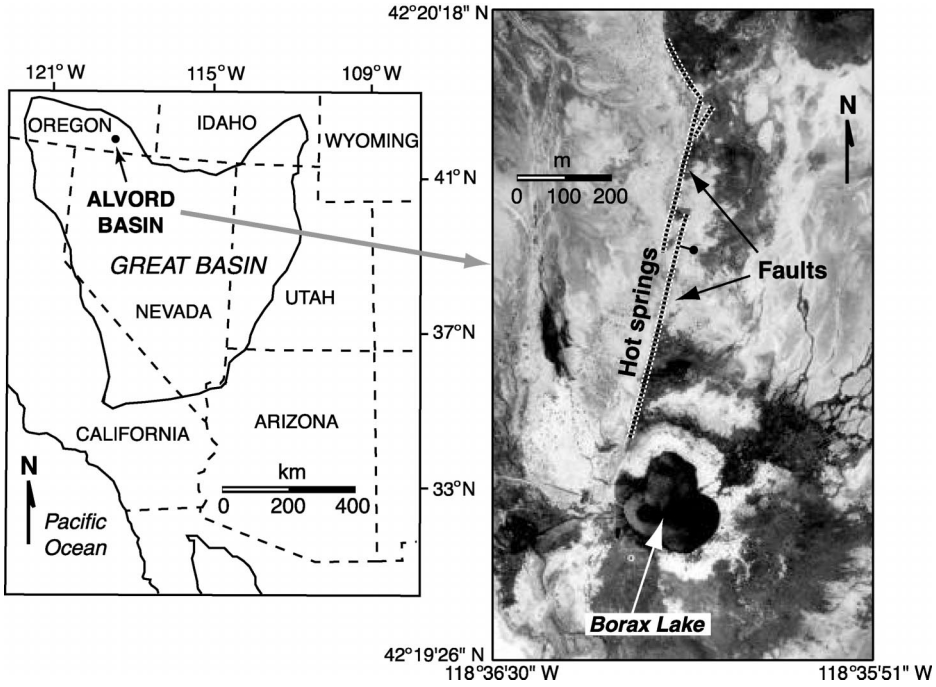

Figure 1. Borax Lake geothermal area is located in southeast Oregon, within Great Basin extensional subprovince of western United States. Aerial photograph shows location of left-stepping en echelon fault system north of Borax Lake that controls occurrence of geothermal springs monitored for this study.

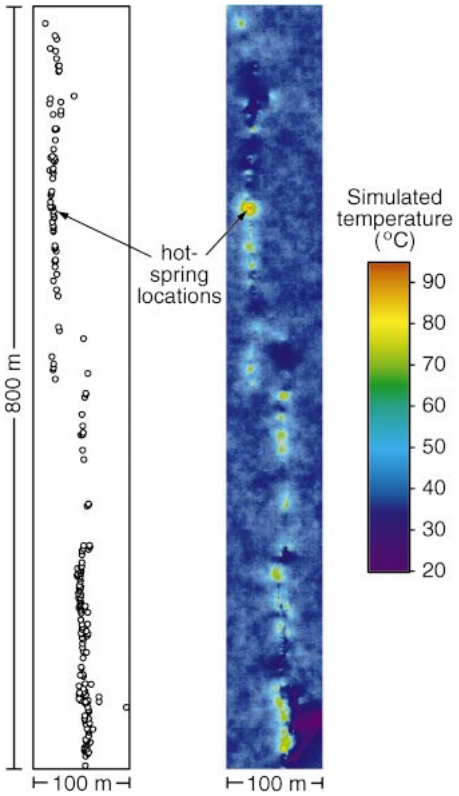

Figure 2. Temperatures shown are composite of 100 equally probable temperature distributions generated by sequential Gaussian simulation (Deutsch and Journel, 1998). Simulations used exponential model of spatial variability and were conditioned to field measurements of temperature taken in Borax Lake fault; locations of spring vents (shown to left of simulated temperature field) clearly delineate trend of fault.

Utah, and Curewitz and Karson (1997) proposed a general conceptual model of fault permeability evolution in hydrothermal discharge zones. In this study we evaluate the hydraulic architecture of an active normal fault controlling hydrothermal discharge near Borax Lake, in southeast Oregon (Fig. 1). Borax Lake is located in the Alvord Basin, a large, complex graben that forms the northeastern extent of the northeast-trending Black Rock–Alvord Basin lineament (Coolbaugh et al., 2003). Mapping of thermal springs in the Borax Lake area shows that geothermal activity is preferentially focused along an active, north-northeast–trending fault that displaces Miocene volcanic rocks and a thin overburden of volcaniclastic sedimentary deposits and late Pleistocene–Quaternary pluvial and playa deposits.

DATA COLLECTION

More than 700 ground and spring temperature measurements were collected with a handheld digital thermometer along a 1 km length of the Borax Lake fault during 2 days in July 2003. Spring temperature measurements used in the analysis were based on three to five measurements per spring, depending on spring size; to minimize the effects of mixing in surface pools, temperatures were measured as close to the vent as possible, and the measurements were averaged. Repeated measurements established the reproducibility of temperatures over the two days of data collection reported in this study. The analysis described here included temperatures representative of 175 geothermal springs, whereas the remaining 527 temperatures were measured in the near-surface materials at varying distances from the geothermal springs. Spring locations were mapped by using radio-linked, dual-frequency Leica global positioning system receivers; ground-temperature measurement locations were determined by using the established spring locations as reference points. Temperatures measured in the fault zone ranged from 21 to 94 °C with a mean of 42.6 °C, although the majority of measurements fell below the average. Individual and mean spring temperatures varied somewhat between data collection efforts (July 2002, March 2003, June 2004, and July 2003), but these variations did not significantly affect the results of the spatial analysis presented here.

GEOSTATISTICAL MODELING AND DATA ANALYSIS

A geostatistical model of temperature in an 800 × 100 m segment of the Borax Lake fault zone was developed from, and conditioned on, the measured temperatures, according to the method outlined in Fairley et al. (2003). In brief, the data were used to develop an experimental variogram, which is a plot of the squared difference in temperature between all spring pairs as a function of their separation distance. The experimental variogram was fit with linear combinations of established mathematical models to obtain a quantitative representation of the experimental data. The resulting model, known as a model variogram, is a mathematical expression of the relationship between physical proximity and temperature variability. For more information regarding the preparation and modeling of variograms, see, for example, Rubin (2003).

The model variogram developed from the Borax Lake temperature data was used to simulate temperature fields at 1 m^2 resolution over an 800 × 100 m segment of the Borax Lake fault. The simulations were generated by using a sequential Gaussian simulation algorithm (Deutsch and Journel, 1998) and conditioned to match exactly the measured temperature data. For the present analysis, the results of 100 simulations were averaged on a pixel-by-pixel basis to develop a composite image of temperatures in a two-dimensional, horizontal plane at the land surface (Fig. 2).

Probability density functions and cumulative density functions (pdfs and cdfs, respectively) from the simulated fault-temperature fields are shown in Figure 3. Not surprisingly,

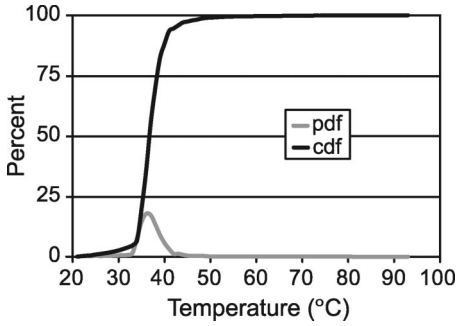

Figure 3. Probability distribution function (pdf; shown in gray) and cumulative distribution function (cdf; shown in black) for temperatures in fault zone were inferred from geostatistical simulations conditioned to ~700 field measurements of temperature.

the simulations show that the majority of the fault is at or near the ambient background temperature in that 55% of the temperatures are between 21 and 37 °C. Of the fault temperatures, ~12% are >40 °C, and ~1% of the total area examined is >50 °C. The highest temperatures in the analysis—between 90 and 94 °C (the highest temperature measured in the field)—occupy <0.01% of the fault area. Because geothermal fluids lose heat to the surrounding environment as they rise to the surface, hotter temperatures generally correspond to higher-permeability flow paths (Forster and Smith, 1989; Wisian, 2000; Fairley et al., 2003). The temperature distribution calculated from the inferred temperature field therefore indicates that fluid moving vertically along fast-flow pathways is restricted to a small fraction of the total area available for flow parallel to the fault, although the exact percentage is determined by the criterion used to define a fast pathway.

Understanding the areal distribution of flow paths in the Borax Lake fault is a significant step toward refining conceptual models of fluid flow in fault zones; however, for many applications it is more important to quantify the fraction of the total flux moving parallel to the fault that is carried by fast pathways. To estimate this quantity from the available data, we used a simple one-dimensional analytical model of heat transport in the Borax Lake fault. The steady-state transport of thermal energy by a convecting fluid is governed by the convection-diffusion equation (CDE; Clark, 1996):

$$\frac{\partial^2 T}{\partial z^2} - \frac{1}{\alpha}\frac{\partial (UT)}{\partial z} = \beta(T - T_\infty). \quad (1)$$

Equation 1 is written to include a term for loss of thermal energy to the surrounding environment at some far-field temperature, T_∞. The variables in equation 1 are fluid velocity (U), fluid temperature (T), and the spatial and temporal coordinate axes (z and t, respectively). The thermal diffusivity of the fluid is represented by α, and β is the coefficient of convective heat transfer divided by the flow-path aspect ratio (length divided by perimeter) times the thermal conductivity of the surrounding geologic medium.

For flow in the Borax Lake fault, the transport of heat by fluid convection dominates over diffusive transport; therefore, the diffusion term of equation 1 (the first term on the left side) can be neglected. If the effective fluid-flow velocity is assumed to be constant, the CDE simplifies to a first-order differential equation that includes a term to account for lateral heat losses between the geothermal reservoir and the land surface. The simplified equation is

$$\frac{dT}{dz} = -\frac{\alpha\beta}{U}(T - T_\infty). \quad (2)$$

The solution of equation 2 provides a description of several quantities of interest, including the fluid flux, the flow velocity, and the effective hydraulic conductivity for a given flow path. Calculating absolute values of flux or conductivity requires knowledge of a number of parameters that are difficult to ascertain and may vary between flow paths; for example, thermal conductivity may vary slightly between the core, the damage zone, and the protolith. The variability of these parameters is generally small compared to their magnitude, however, and a robust estimate of the hydraulic conductivity distribution in the fault is readily obtained by comparing individual flow paths against a reference case if the initial temperature is assumed constant for all flow paths. The assumption of constant initial temperature appears reasonable for the Borax Lake fault springs on the basis of (1) standard geothermometers and (2) geochemical data that indicate a common source for all the springs sampled (Cummings et al., 1993). This approach allowed property distributions to be calculated without requiring values to be specified for α and β, which are poorly constrained. For our analysis, we selected a reference temperature of 36.0 °C. All flow paths with temperatures at the land surface equal to 36.0 °C were therefore assigned a value of 1.0; flow paths with land-surface temperatures of >36.0 °C were assigned values of hydraulic conductivity of >1.0, as determined by the formula

$$\frac{K}{K_0} = \frac{\ln(1 - \theta_0)}{\ln(1 - \theta)}, \quad (3)$$

where the subscript 0 indicates the reference case, K is the effective hydraulic conductivity of the flow path (L/T), and θ is the temperature measured at the land surface (T) normalized against the temperature in the geothermal reservoir (T_r) and the environmental temperature far from the fault (T_∞) according to

$$\theta = \frac{T - T_r}{T_\infty - T_r}. \quad (4)$$

Because all flow paths are assumed to have been initiated from the same hydraulic head, ratios of hydraulic conductivity developed in the analysis are equally representative of flux in the individual flow pathways.

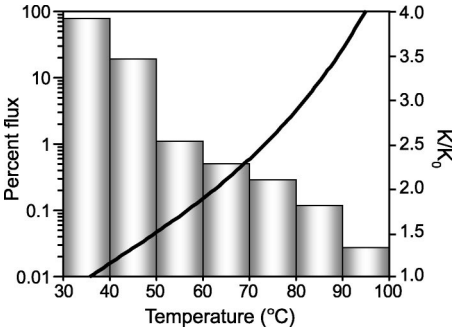

Figure 4. Flux-temperature relationships for flow paths parallel to plane of Borax Lake fault. Line plot shows ratio of flow path hydraulic conductivity (K) to hydraulic conductivity of reference flow path (K_0) as function of temperature measured at land surface. Histogram gives total flux in fault partitioned into categories based on temperatures at land surface. Percentage of flux transmitted by flow paths of given temperature range is derived relative to reference land-surface temperature of 36 °C. All flow paths are assumed to have been initiated from location having temperature of 155 °C (consistent with Cummings et al., 1993) and to cool toward far-field environmental temperature averaging 26 °C. Note logarithmic ordinal axis.

DISCUSSION AND CONCLUSIONS

The pdfs and cdfs representing the distribution of flux in the fault are similar in shape to those from the temperature analysis shown in Figure 3, but differ in a somewhat nonlinear fashion owing to the presence of the natural logarithms in equation 3. The relationship between discharge temperature and flux is shown in Figure 4, along with a histogram of flux in increments of 10 °C. The analysis shows that a higher-temperature flow path carries a proportionately greater amount of flux than a flow path near the reference value; however, Figure 4 clearly illustrates that the contribution of fast-flow paths in the fault zone is negligible in comparison to the total vertical flux transported parallel to the fault, simply by virtue of the limited areal extent of the fast pathways. This finding is true regardless of the criterion used to define fast flow.

For example, a conservative criterion such as flow paths demonstrating land-surface temperatures of >50 °C results in only slightly more than 2% of the total flux in the fault being carried by fast pathways; a more realistic criterion—such as flow paths with land-surface temperatures of >70 °C—credits fast pathways with transmitting ~0.5% of the total flux.

The hydraulic structure analysis for an active, extensional fault in the Great Basin is an important step for refining conceptual models of fault hydraulic architecture. Although our analysis was made possible by the unique character of the fault-controlled geothermal system at Borax Lake, we expect the observed distributions of hydraulic properties and fluid flux to apply in a general sense to a wide variety of fault settings; further, our findings may provide a useful test case for studies in areas such as fluid-induced tectonic activity, petroleum migration, ore mineralization, and fluid circulation in geothermal systems.

ACKNOWLEDGMENTS

We thank J. Heffner, L. Tumlinson, N. Raterman, and T. Williams for assistance in data collection and analysis and K. Whipple and E. Singleton for mapping support. We also thank P. Dobson and Y. Geraud for helpful comments and suggestions. This work was funded by National Science Foundation grant EPS-0132626.

REFERENCES CITED

Barton, C.A., Zoback, M.D., and Moos, D., 1995, Fluid flow along potentially active faults in crystalline rock: Geology, v. 23, p. 683–686.

Blewitt, G., Coolbaugh, M., Sawatzky, D., Holt, W., Davis, J., and Bennett, R., 2003, Targeting of potential geothermal resources in the Great Basin from regional to basin-scale relationships between geodetic strain and geological structures, *in* Proceedings, Annual GRC Meeting, Morelia, Mexico, October 12–15, 2003: Davis, California, Geothermal Resources Council Transactions, v. 27, p. 3–7.

Bruhn, R.L., Yonkee, W.A., and Parry, W.T., 1990, Structural and fluid-chemical properties of seismogenic normal faults: Tectonophysics, v. 175, p. 139–157.

Bruhn, R.L., Parry, W.T., Yonkee, W.A., and Thompson, T., 1994, Fracturing and hydrothermal alteration in normal fault zones: Pure and Applied Geophysics, v. 142, p. 609–644.

Caine, J.S., Evans, J.P., and Forster, C.B., 1996, Fault zone architecture and permeability structure: Geology, v. 24, p. 1025–1028.

Campbell, K., Wolfsberg, A., Fabryka-Martin, J., and Sweetkind, D., 2003, Chlorine-36 data at Yucca Mountain: Statistical tests of conceptual models for unsaturated-zone flow: Journal of Contaminant Hydrology, v. 62–63, p. 43–61.

Clark, M.M., 1996, Transport modeling for environmental engineers and scientists: New York, John Wiley and Sons, 559 p.

Coolbaugh, M.F., Sawatzky, D.L., Oppliger, G.L., Minor, T.B., Raines, G.L., Shevenell, L.A., Blewitt, G., and Louie, J.N., 2003, Geothermal GIS coverage of the Great Basin, USA: Defining regional controls and favorable exploration terrains, *in* Proceedings, Annual GRC Meeting, Morelia, Mexico, October 12–15, 2003: Davis, California, Geothermal Resources Council Transactions, v. 27, p. 9–11.

Cummings, M.L., St. John, A.M., and Sturchio, N.C., 1993, Hydrogeochemical characterization of the Alvord Basin geothermal area, Harney County, Oregon, USA, *in* Proceedings, 15th New Zealand Geothermal Workshop: Auckland, New Zealand, Geothermal Institute, University of Auckland, p. 119–124.

Curewitz, D., and Karson, J.A., 1997, Structural settings of hydrothermal outflow: Fracture permeability maintained by fault propagation and interaction: Journal of Volcanology and Geothermal Research, v. 79, p. 149–168.

Deutsch, C.V., and Journel, A.G., 1998, GSLIB geostatistical software library and user's guide: Oxford, Oxford University Press, 384 p.

Evans, J.P., Forster, C.B., and Goddard, J.V., 1997, Permeability of fault-related rocks, and implications for hydraulic structure of fault zones: Journal of Structural Geology, v. 19, p. 1393–1404.

Fabryka-Martin, J.T., Flint, A.L., Sweetkind, D.S., Wolfsberg, A.V., Levy, S.S., Roemer, G.J.C., Roach, J.L., Wolfsberg, L.E., and Duff, M.C., 1997, Evaluation of flow and transport models of Yucca Mountain, based on chlorine-36 studies for FY97: Los Alamos, New Mexico, Los Alamos National Laboratory Report LA-CSS-TIP-97-010.

Fairley, J., Heffner, J., and Hinds, J., 2003, Geostatistical evaluation of permeability in an active fault zone: Geophysical Research Letters, v. 30, no. 18, 1962, doi: 10.1029/2003GL018064.

Forster, C., and Smith, L., 1989, The influence of groundwater flow on thermal regimes in mountainous terrain: A model study: Journal of Geophysical Research, v. 94, p. 9439–9451.

Jourde, H., Flodin, E.A., Aydin, A., Durlofsky, L.J., and Wen, X.-H., 2002, Computing permeability of fault zones in eolian sandstone from outcrop measurements: American Association of Petroleum Geologists Bulletin, v. 86, p. 1187–1200.

Kiguchi, T., Ito, H., Kuwahara, Y., and Miyazaki, T., 2001, Estimating the permeability of the Nojima fault zone by a hydrophone vertical seismic profiling experiment: The Island Arc, v. 10, p. 348–356.

Koenig, J.B., and McNitt, J.R., 1983, Controls on the location and intensity of magmatic and non-magmatic geothermal systems in the Basin and Range province: Geothermal Resources Council Special Report 13, 93 p.

Olsen, M.P., Scholz, C.H., and Léger, A., 1998, Healing and sealing of a simulated fault gouge under hydrothermal conditions: Implications for fault healing: Journal of Geophysical Research, v. 103, p. 7421–7430.

Pezzopane, S.K., and Weldon, R.J., 1993, Tectonic role of active faulting in central Oregon: Tectonics, v. 12, p. 1140–1169.

Rawling, G.C., Goodwin, L.B., and Wilson, J.L., 2001, Internal architecture, permeability structure, and hydrologic significance of contrasting fault-zone types: Geology, v. 29, p. 43–46.

Rubin, Y., 2003, Applied stochastic hydrogeology: Oxford, Oxford University Press, 416 p.

Seront, B., Wong, T.-F., Caine, J.S., Forster, C.B., Bruhn, R.L., and Fredrich, J.T., 1998, Laboratory characterization of hydromechanical properties of a seismogenic normal fault system: Journal of Structural Geology, v. 20, p. 865–881.

Wisian, K.W., 2000, Insights into extensional geothermal systems from numerical modeling, *in* Proceedings, World Geothermal Congress, Kyushu-Tohoku, Japan: Pisa, Italy, International Geothermal Association, p. 1947–1952.

Wisian, K.W., Blackwell, D.D., and Richards, M., 1999, Heat flow in the western United States and extensional geothermal systems, *in* Proceedings, 24th Workshop on Geothermal Reservoir Engineering, Stanford, California, January 25–27, 1999: Stanford, California, Stanford Geothermal Program, p. 219–226.

Manuscript received 26 February 2004
Revised manuscript received 11 May 2004
Manuscript accepted 17 May 2004

Printed in USA